JBC Papers in Press. Published on June 1, 2009 as Manuscript M109.018804
The latest version is at http://www.jbc.org/cgi/doi/10.1074/jbc.M109.018804

# Plasminogen Activator Inhibitor-1 Regulates Integrin αvβ3 Expression and Autocrine TGFβ Signaling.

**Benjamin S. Pedroja[1], Leah E. Kang[1], Alex O. Imas[1], Peter Carmeliet[2,3], and Audrey M. Bernstein[1]**

[1]Department of Ophthalmology, Mount Sinai School of Medicine, New York, NY. [2]Vesalius Research Center (VRC), VIB, 3000 Leuven, Belgium, [3]Vesalius Research Center (VRC), K.U.Leuven, 3000 Leuven, Belgium.

Running Head: PAI-1 regulates αvβ3 integrin and TGFβ activity

Address Correspondence to: Dr. Audrey Bernstein, Mount Sinai School of Medicine, Box 1183, 1 Gustave L. Levy Place, New York, NY 10029. Fax: 212-289-5945.
E-mail: audrey.bernstein@mssm.edu

**Fibrosis is characterized by elevated TGFβ signaling resulting in extracellular matrix accumulation and increased PAI-1 (plasminogen activator inhibitor) expression. PAI-1 induces the internalization of uPA/uPAR (urokinase plasminogen activator/ receptor) and integrin αvβ3 from the cell surface. Since increased αvβ3 expression correlates with increased TGFβ signaling, we hypothesized that aberrant PAI-1-mediated αvβ3 endocytosis could initiate an autocrine-loop of TGFβ activity. We found that in PAI-1 KO mouse embryonic fibroblasts (MEFs), αvβ3 endocytosis was reduced by ~75%, leaving αvβ3 in enlarged focal adhesions, similar to WT cells transfected with PAI-1 siRNA. TGFβ signaling was significantly enhanced in PAI-1 KO cells as demonstrated by a 3-fold increase in SMAD 2/3 containing nuclei and a 2.9-fold increase in TGFβ activity that correlated with a 2.5-fold increase in αvβ3 and TGFβRII expression. As expected, PAI-1 KO cells had unregulated plasmin activity, which was only partially responsible for TGFβ activation as evidenced by a mere 25% reduction in TGFβ activity when plasmin was inhibited. Treatment of cells with an αvβ3-specific cyclic RGD peptide (GpenGRGD) led to a more profound (59%) TGFβ inhibition; a non-specific RGD peptide (GRGDNP) inhibited TGFβ by only 23%. Human primary fibroblasts were used to confirm that PAI-1 inhibition and β3 over-expression led to an increase in TGFβ activity. Consistent with a fibrotic phenotype, PAI-1 KO cells were constitutively myofibroblasts that had a 1.6 fold increase in collagen deposition over WT cells. These data suggest that PAI-1-mediated regulation of αvβ3 integrin is critical for the control of TGFβ signaling and the prevention of fibrotic disease.**

Fibrotic disorders can result from environmental toxins, persistent infection, autoimmune disease or mechanical injury, leading to the hardening and scarring of tissues. In fibrotic diseases such as liver cirrhosis, renal fibrosis, and idiopathic lung fibrosis, or in pathological wound healing such as hypertrophic scarring, scleroderma, and Dupuytren's disease, the persistence of myofibroblasts contributes to disease progression by overproduction of extracellular matrix (ECM) and by excessive contraction (1-3). A shift in the balance of growth factors and cytokines that promote ECM deposition and proteases that degrade matrix often contributes to fibrotic disease (4,5). Plasmin, a broad-spectrum protease that is generated from plasminogen by uPA is one of the proteases that degrades matrix, activates growth factors and other proteases (6). Since uPA activity is inhibited by PAI-1, the over-expression of PAI-1 results in matrix accumulation. For this reason, PAI-1 is a key prognostic marker for fibrotic disease. PAI-1 exerts its inhibitory activity on uPA by stimulating the endocytosis of the cell-surface uPA/uPAR complex through the low-density lipoprotein receptor-related protein (LRP receptor) (7). Integrin αvβ3 is also internalized with the uPA/uPAR/LRP complex (8). After endocytosis, uPAR and integrins are recycled back to the cell surface for another round of binding (8,9). uPAR and αvβ3 promote cellular

attachment and spreading, as they are receptors for the extracellular matrix molecule, vitronectin (10). Thus, cycling of the complex is thought to stimulate the attachment and detachment that is necessary for cell migration (8). Consequently, a shift in the expression of any of these components (PAI-1/uPA/uPAR/αvβ3) can result in either aggressive migration, as seen in cancer invasion or a persistent increase in cell adhesion and cell tension, as seen in myofibroblasts in fibrotic tissue.

The family of TGFβ growth factors has been intensively studied for their role in fibrotic wound healing. Upregulation of TGFβ results in amplified and persistent over-production of molecules such as integrins and PAI-1 and other protease inhibitors (e.g. TIMPs) (2,3). Upregulated integrins continue the cycle of TGFβ signaling by participating in the sustained activation of TGFβ from its latent form. To date, studies have found that various αv-integrins participate in the activation of TGFβ (αvβ3, αvβ5, αvβ6, and αvβ8) but the mechanism differs (11-15). Integrins can serve as docking proteins to localize proteases that cleave and activate latent-TGFβ in the ECM or they can directly activate latent-TGFβ in a protease-independent manner. Recently it was discovered that latent-TGFβ is also activated by mechanical stress generated from an integrin-mediated interaction between myofibroblasts and the ECM, primarily involving αvβ5. The mechanical stress promotes a conformational change that activates the latent-TGFβ complex (15). αv integrins also modulate TGFβ signaling through the binding of αvβ3 to TGFβ Receptor II (TGFβRII) in the presence of TGFβ. This interaction was shown to promote a dramatic increase in the proliferation of lung fibroblasts and induce invasion of epithelial breast cancer cells (16,17).

Our data establish a role for the PAI-1-mediated control of αvβ3 expression and support a significant role for αvβ3 in TGFβ signaling. Using PAI-1 KO cells we tested the hypothesis that the absence of PAI-1 would result in the accumulation of αvβ3 on the cell surface since PAI-1 promotes the endocytosis of uPA/uPAR/αvβ3. PAI-1-mediated endocytosis of β3 was significantly reduced in the PAI-1 KO cells. Correspondingly, we report that β3 accumulated at the cell surface in enlarged β3–containing focal adhesions. Thus we explored whether the accumulation of αvβ3 on the cell-surface had fibrogenic effects even in the absence of pro-fibrotic PAI-1. Our results demonstrate dramatically increased TGFβ activity and an increase in collagen expression in PAI-1 KO cells. Together these findings suggest that PAI-1 modulates β3 expression and localization, and in turn, TGFβ signaling. Our data reveal that maintaining precise levels of PAI-1 are a key to preventing fibrosis. Understanding the consequence of regulating PAI-1 activity is critical in light of the many clinical therapies currently under development that target PAI-1 (18,19).

## EXPERIMENTAL PROCEDURES

*Antibodies, reagents and cells:* Transformed Mink Lung Epithelial Cells (TMLC) containing the PAI-1 promoter fused to the luciferase gene were a generous gift of Dr. Daniel Rifkin, New York University, NY, NY. Antibodies to integrin β3 (R36) used for immunoflourescence were a generous gift of Dr. Barry Coller, Rockefeller University, NY, NY. Anti-vimentin antibody was a generous gift of Dr. Paul FitzGerald, University of California, Davis, CA. Antibodies against mouse PAI-1 were from American Diagnostica (sheep) and R&D (rat), and TGFβRII (ab28382) were from Abcam, Cambridge, MA, β3 antibody used for immunoprecipitation and western blotting (ab1932) was from Chemicon, Billerica, MA, β3 antibody (16-0611) and hamster IgG (16-4888) used for the endocytosis assay were from eBioscience, San Diego CA, anti-early endosome antigen 1 (EEA1) antibody was from Abcam (ab15846-200), SMAD 2/3 antibody was from BD Biosciences, San Jose, CA, SMAD-2, SMAD-3, phospho-SMAD2, and phospho-SMAD3 antibodies were from Cell Signaling, Danvers, MA, and vinculin antibody was from Sigma, St. Louis, MO. Anti-α-SMA antibody was from Sigma. FITC labeling kit was from Novus Biologicals, Littleton, CO. Secondary Alexa-488 and Alexa-568 were from Molecular

Probes, Eugene, Oregon. HRP-conjugated anti-Streptavidin antibodies and all HRP-conjugated secondary antibodies were from Jackson Laboratories, Bar Harbor, Maine. Mouse PAI-1 siRNAs were from Santa Cruz Biotechnologies, Santa Cruz, CA and the non-targeting fluorescent nucleotide control (siGlo) was from Dharmacon, Lafayette, CO. Human β3 cDNA (pcDNA3) was a generious gift from Dr. Peter Newman, Blood Research Institute, Blood Center of Wisconsin, Milwaukee, WI and the GFP construct (EGFP-C1) was from Clontech, Mountain View, CA. Aprotonin was from Calbiochem, San Diego, CA. The control RGD peptide (GRGDNP) was from Biomol, Plymouth Meeting, PA, and the cyclic-RGD peptide (GpenGRGD) was from Bachem, Torrance, CA. Collagen (PureCol) was from Inamed, Fremon, CA and vitronectin was from Sigma.

*Cells and media:* PAI-1 MEFs were maintained in PAI-1 complete media: DMEM (Invitrogen) with 10% FCS (Hyclone, Logan, UT), 1mM L-Glutamine, 1X MEM non-essential amino acids (Invitrogen), and pen-strep (Sigma). For experiments except where noted cells were plated on 10ug/ml collagen in supplemented serum-free media (SSFM): DMEM, 1X RPMI-1640 Vitamin Mix, 1X ITS Liquid media supplement**,** 1μg/ml glutathione; (all from Sigma), 2mM L-glutamine, 1mM sodium pyruvate, 0.1 mM MEM non-essential amino acids; (Invitrogen) with pen-strep.

Human primary corneal fibroblasts (HCF) were derived from the stroma of human corneas that were not suitable for transplantation (obtained from NDRI, Pittsburgh, PA). Stromal fibroblasts were isolated as previously described (20).

*Immunocytochemistry:* Cells were fixed with 3% p-formaldehyde (Fisher Scientific, Fair Lawn, NJ) and permeabilized with 0.1% Triton X-100 (Sigma). After blocking with 3% normal mouse serum (Jackson Immuno Research), cells were incubated with primary antibody (anti-αvβ3 (R36), anti-vinculin, anti-SMAD 2/3, anti-SMAD 3, or anti-α-SMA) washed in PBS, and incubated with secondary antibodies (Alexa-488 or Alexa-568). Coverslips were viewed with an Zeiss Axioskop microscope and images were captured using a Zeiss Axioscope with a SPOT-2 CCD camera (Diagnostic Instruments, Sterling Heights, Michigan) and processed by Adobe PhotoShop software.

*Western blots:*24 hours after seeding, cells were detached with Detachment Buffer (20 mM Tris, pH 7.5, 250 mM sucrose), pelleted, and lysed in 1% SDS plus complete protease inhibitor tablet (Roche), phenylmethylsulfonyl fluoride (PMSF, Sigma), $Na_3VP_4$ (Fisher) and benzonase (Sigma). 30μg of protein was separated on 4-12% NuPAGE gradient gels and transferred to nitrocellulose membranes (gel for αvβ3 was non-reducing, gels for TGFβRII ,vimentin, SMAD 2 and 3, and pSMAD2 and 3 were reducing). For anti-αvβ3, streptavidin-HRP and pSMAD 2 and 3, blots were processed with 5% BSA in TBS. TGFβRII, PAI-1, vimentin, SMAD 2 and 3 blots were blocked with 5% milk in Tris-buffered saline (TBS). Primary and secondary antibodies conjugated to HRP were diluted in BSA or milk, correspondingly. Bands were visualized with ECL (Pierce).

*Immunoprecipitation (IP):* For cell-surface expression, cells were biotinylated for 30 minutes with 0.5mg/ml EZ-Link Sulfo-NHS-LC-Biotin (Pierce) prior to detachment with Detachment buffer. For αvβ3 IP, cell pellets were lysed in Triton Buffer (1% Triton, 150mM NaCl, 20mM Tris, 1mM $MgCl_2$, 1mM $CaCl_2$, 10% Glycerol pH 7.5) plus protease inhibitors (as above). For TGFβRII cell pellets were lysed in 1% SDS (Fisher), plus protease inhibitors. SDS lysates were diluted to 0.1% SDS for protein determination and IPs. For each IP, protein A or G beads (Upstate) and 5ug of antibody were added to 0.5 mg of total protein and incubated overnight at 4°C. Eluted proteins were separated under reducing conditions, and transferred to nitrocellulose before blocking with BSA and incubation with streptavidin-HRP. Bands were visualized with ECL (Pierce). For PAI-1 IP, Triton lysates were IPed with anti-PAI-1 (American Diagnostica) and detected with anti-PAI-1 (R&D).

*Endocytosis Assay:* PAI-1 WT and KO cells were seeded in PAI-1 complete media at $1X10^4$ cells/ml. FITC-labeled anti-β3 antibody and FITC-labeled control IgG (both without azide) (ebioscience) were incubated in 0.5% FBS in DMEM for 30 min at 37°C before fixation with

p-formaldehyde. Cells were then co-immunostained for early endosome antigen 1 (EEA1) to identify early endosomes. Autoflouresence was not quenched in this procedure to maintain the endocytosed FITC signal. MetaMorph® image analysis software was used to quantify overlap between β3 and EEA1.

*Transfections:* Transient transfection was performed using the Amaxa Nucleofection® system (Gaithersburg, MD). PAI-1 MEFs were transfected using the MEF2 kit with either 1μM siRNA and 1μg of EGFP plasmid or EGFP alone and cells were seeded in PAI-1 complete media, without antibiotics. HCFs were co-transfected with 1μM human PAI-1 siRNA, 1μM siGlo, 2.5μg human β3 cDNA with 2.5μg EGFP plasmid, or EGFP alone, using the NHDF kit and seeded in HCF complete media without antibiotics. Axiovert images were captured with an Axiocam MRm CCD camera.

*RNA Extraction and qPCR: Total* RNA was extracted from cell lysates using the RNeasy kit (Qiagen). First stranded cDNA was generated from 200ng of total RNA using the Omniscript RT kit (Qiagen) and random primers (Invitrogen) according to the manufacturer's instructions. Triplicate determinations were analyzed by qPCR using the $RT^2$ Real-time detection system (SuperArray, Frederick, MD) and ABI 7900 sequence detection system. Annealing temperature was 55°C for all reactions. Primers used were mouse PAI-1 forward 5'- GGGGTAGGTTGGGAGAATGT -3' and reverse 5'-TCTGGGACAAAGGCTAAGGA -3', human β3 forward 5'-TCACCAGTAACCTGCGGATTG-3' and reverse 5'-GTAGCCAAACATGGGCAAGC-3'. Primers for Human PAI-1, human β-actin, and mouse β-actin were obtained from realtimeprimers.com, Elkins Park, PA.

*PA activity assay:* This assay was performed as previously described (20). Briefly, cells were plated onto collagen or vitronectin in SSFM alone or with, 1ng/ml FGF-2 (Invitrogen) and 1ug/ml heparin (Fisher), or with 1ng/ml TGFβ1 (R&D) and grown for 24 hours. After cell lysis, uPA activity was determined using a chromogenic substrate for plasmin (Spectrozyme PL, American Diagnostic). The reaction product was measured on a Biotek spectrophotometer (A405 nm) at 1 hour.

*TGFβ Activity Assay:* This protocol was slightly modified from previously published assays (12,21). PAI-1 cells were co-cultured with Transformed Milk Lung Epithelial Cells (TMLC), which contain the PAI-1 promoter fused to the luciferase gene. PAI-1 WT or KO MEFS and TMLC were plated at 1 x $10^5$ cells per well (each) in 24 well dishes in DMEM, 10% FBS, 1mM L-Glutamine, and pen-strep. After 24 hours the media were replaced with (0.1% BSA in DMEM, pen-strep) and incubated for 24 hours. Luciferase activity was measured in triplicate using the Bright-Glo detection system (Promega) and luminescence was determined using a Synergy 2 Biotek Microplate Reader (Winooski, VT). To determine the contribution of plasmin to TGFβ activity, 10ug/mL of aprotinin was added when cells were seeded and re-added when the medium was changed. Similarly for the peptide inhibition experiment 100nM of either control GRGDNP or cyclic-RGD peptide, GpenGRGD was re-added when the medium was changed. In addition, cells were plated on 10ug/ml of collagen to prevent cell detachment when peptides were added. PAI-1 siRNA and β3 transfected HCFs were co-cultured with TMLC cells and assayed for luciferase activity as described above.

*Quantitative assay for collagen synthesis:* This assay was performed as per (22). Briefly, $1X10^5$ PAI-1 WT and KO cells were seeded in PAI-1 complete media into 24-well dishes and grown for 2 days before fixation in Boulin's Fixative (75% Picric Acid (Sigma), 20% formaldehyde, 5% glacial acetic acid (Fisher). Cells were washed and dried overnight at RT. To stain for collagen synthesis, Sirius Red stain (0.25 gm Direct Red (Sigma), 250 ml Picric Acid) was added per well for 1 hr. Wells were washed with 0.01N HCl (Fisher) and dye was eluted with 0.5ml of 0.1N NaOH (Fisher). Duplicate points (150ul) from triplicate wells were read at A550 on a Synergy 2 Biotek Reader in a 96-well plate. After elution, wells were washed and air-dried. Cell count was determined with Crystal Violet (Fisher). To determine the amount of collagen

synthesis per cell, the ratio of Sirus Red to Crystal violet was calculated.
*Statistical Analysis:* Each experiment was repeated three to six times. Numerical data are expressed as the mean +/- standard deviation.

## RESULTS

To confirm that PAI-1 KO MEFs lacked PAI-1, lysates of WT and KO cells were immunoprecipitated (IPed) with anti-PAI-1 antibody. These data confirm the presence of PAI-1 in WT cells and its absence from KO cells (Figure 1A). As expected, PAI-1 KO lysate did not yield a signal for PAI-1 despite equal loading of protein.

*Endocytosis of β3 in PAI-1 KO cells is significantly reduced.* To determine if PAI-1 KO cells had reduced endocytosis of β3, PAI-1 WT and KO cells were incubated with FITC labeled anti-β3 antibody that binds to a cell-surface epitope of β3. After 30 minutes at 37°C cells were fixed and co-stained with an antibody to the early endosome protein (EEA1). Whereas WT cells have significant co-localization between β3 and EEA1 (Figure 1B, top left, yellow punctate dots), KO cells have very few co-localizing endocytic vesicles (Figure 1B, top right). FITC-labeled IgG was used as control (bottom panels). Neither the WT nor KO cells showed a dramatic uptake of the control IgG. Overlap between β3 and control IgG with EEA1 were quantified using Metamorph Analysis (Figure 1C). Of note is that the FITC-β3 does not accumulate in focal adhesions under these conditions (see Figure 3 for focal adhesion staining). Instead, the antibody/integrin complex is internalized into endocytic vesicles. These data suggest that PAI-1 KO cells have impaired endocytosis of β3. Next we determined if impaired endocytosis of β3 resulted in an accumulation of β3 on the cell surface of PAI-1 KO cells.

*PAI-1 KO cells displayed significantly increased cell-surface expression of β3 and TGFβRII.* Previously, PAI-1 was shown to promote the endocytosis of αvβ3 through a uPA/uPAR mediated mechanism (8). To determine if there was an increase of αvβ3 on the cell surface of PAI-1 KO cells, WT and KO cells were cell-surface biotinylated before lysing and IPing with antibodies to β3. Resultant western blots were probed with streptavidin-HRP revealing specific bands whose integrin identity was determined by molecular weight. Figure 2A shows that αvβ3 expression was increased on the cell surface. Since β3 participates in the activation of TGFβ (11,12), and increased TGFβ activity is associated with over-expression of TGFβRII in models of fibrosis (23,24), we investigated if TGFβRII was upregulated on the cell surface of PAI-1 KO cells. Indeed, as with αvβ3, TGFβRII cell-surface expression was increased in KO cells. Similar to the cell-surface expression of αvβ3 and TGFβRII, western blots showed that total expression was greatly enhanced in lysates of PAI-1 KO cells (Figure 2B). Mechanistically, β3 cell-surface over-expression could increase TGFβ signaling by directly activating latent-TGFβ in the matrix and/or by constitutively binding to the TGFβRII, and over-expression of TGFβRII would enhance this binding. Both pathways would sustain TGFβ signaling trapping the cells in an autocrine loop of TGFβ activation. Many attempts were made by IP to detect endogenous binding between αvβ3 and TGFβRII, however this interaction could not be captured using available reagents. Next we determined if impaired endocytosis of β3 changed not only the expression levels of β3 but also the localization of β3 in focal adhesions.

*β3-containing focal adhesions in PAI-1 KO cells are larger and more extensive*. β3-containing focal adhesions in PAI-1 WT and KO cells were compared by epifluorescence microscopy. Figure 3 shows that PAI-1 WT cells (A) have smaller β3-containing focal adhesions compared to KO cells (B), which have large and extended focal adhesions. Since vinculin is a basic component of focal adhesions (25), we used anti-vinculin antibody to confirm the altered organization of focal adhesions in the WT and KO cells (Figure 3, denoted with * and **, respectively**).** Relative focal adhesion size was quantified demonstrating that focal adhesions in KO cells were approximately 2-fold larger than in WT cells (C). Further, PAI-1

WT cells transfected with PAI-1 siRNA produced focal adhesions that were similar to those in PAI-1 KO cells (E) compared to control (D), confirming the specificity of the result. qPCR for PAI-1 showed a 60% decrease in PAI-1 RNA confirming the effect of PAI-1 siRNA transfection in WT cells (F). Again, focal adhesion size in the PAI-1 siRNA containing cells showed a 2-fold increase in size compared to WT cells with GFP alone (G). Together these data show that the absence of PAI-1 produces enlarged focal adhesions containing β3.

*SMAD 2/3 is localized to the nucleus in PAI-1 KO cells***.** TGFβ1 elicits its biological effects by interacting with TGFβRII, which recruits and activates TGFβRI. Activated TGFβRI phosphorylates SMAD2 and SMAD3, which forms a complex with SMAD4 and translocates to the nucleus to elicit gene transcription (26). Thus, the localization of SMAD2/3 to the nucleus is an indicator of TGFβ signaling. In WT and KO cells the localization of SMAD 2/3 to the nucleus was compared. Previous studies demonstrating the binding of β3 with TGFβRII in the presence of TGFβ1, also showed that TGFβ signaling was enhanced in the presence of vitronectin (16). Thus to determine if vitronectin played a role in SMAD 2/3 localization, cells plated on collagen were compared to cells plated on vitronectin. The results demonstrate that PAI-1 KO cells had significantly higher endogenous TGFβ activity than WT cells, approximately 3-fold more nuclear SMAD2/3 on collagen and 3.5 fold more nuclear SMAD2/3 on vitronectin (Figure 4A, left).

To determine the impact of exogenous TGFβ on SMAD2/3 localization, after 24 hours in SSFM, cells were treated with TGFβ1 for 1 hour prior to cell fixation (Figure 4A, right). As expected, at 1 hour, both WT and KO cells responded to exogenous TGFβ addition with 80% nuclear localization of SMAD2/3 on collagen and 100% on vitronectin for WT cells. Because of the enhanced basal level of SMAD2/3 signaling in the KO cells, cells grown on either matrix have 100% nuclear SMAD2/3. The increased TGFβ signaling on vitronectin suggests that the interaction between β3 and TGFβRII may contribute to the TGFβ signaling in these cells. Experiments were repeated with anti-SMAD 3 antibody with similar results (data not shown). Representative images of SMAD2/3 localization are shown in Figure 4B. To confirm the SMAD 2/3 localization data, western blots were performed using antibodies to SMAD 2 and SMAD 3, and their activated forms, phospho-SMAD 2, and phospho-SMAD 3. Results support those reported in Figure 4A and B. Both phospho-SMAD 2 and 3 were significantly increased in PAI-1 KO cells (Figure 4C).

*PA activity is unregulated in PAI-1 KO cells.* Plasmin activates proteases and growth factors including TGFβ from the latent-TGFβ complex. Since PAI-1 is the primary inhibitor of uPA activity, it follows that the absence of PAI-1 would result in unregulated (increased) uPA activity and in turn, unregulated plasmin. To confirm this, a standard assay for PA activity was performed. This colorimetric assay quantifies the generation of plasmin. Previous work from our lab and others have shown that in fibroblasts, FGF-2 increases uPA activity and TGFβ decreases this activity, due to the induction of PAI-1 by TGFβ (20,27,28). In WT cells, FGF-2 stimulated PA activity, whereas TGFβ reduced it by approximately 50%. In contrast, in PAI-1 KO cells, PA activity was equally high in cells grown with FGF-2 or with TGFβ1 (Figure 5A).

*Unregulated plasmin activity is only partially responsible for the TGFβ activity in PAI-1 KO cells*. To investigate if high levels of plasmin were principally responsible for the increase in TGFβ activity in KO cells, we performed a TGFβ activity bioassay that utilizes the induction of the luciferase gene fused to a PAI-1 promoter in TMLC cells (12,21). Active TGFβ was quantified by co-culturing PAI-1 WT and KO cells with TMLC cells containing the lucerifase-PAI-1 construct. We found a 2.9-fold increase in TGFβ activity in KO over WT cells. When we inhibited plasmin activity by performing the assay in the presence of aprotinin, we found only a 25% decrease in TGFβ activity in both WT and KO cells (Figure 5B). (Aprotinin was shown to abolish plasmin activity in the PA activity assay, data not shown). These data demonstrate that plasmin is

playing a role in TGFβ activation but that the majority of the TGFβ signaling can be attributed to other factors. Next we investigated the importance of increased β3 expression to TGFβ activity.

*Inhibition of αvβ3 significantly decreases TGFβ activity***.** To determine if disrupting β3 interactions would affect TGFβ activity, a cyclic peptide that is specifically interferes with β3/RGD binding was utilized in the TGFβ activity assay (29). Although the RGD motif is contained in the ligands for both β1 and β3 integrins, such as latent-TGFβ and ECM, this cyclic RGD peptide (GpenGRGD) preferentially disrupts β3/RGD binding (29), whereas the general RGD peptide (GRGDNP) preferentially disrupts β1/RGD binding (30,31). In our assay, the cyclic peptide reduced TGFβ activity by 59%, whereas the RGD peptide reduced activity by only 23% (Figure 6A). These data provide evidence that β3 accumulation preferentially promotes TGFβ signaling. Futhermore, these date are consistent with a previous report that the cyclic RGD peptide but not the RGD peptide inhibits TGFβ-signaling resulting from αvβ3/TGFβRII binding (16).

*Over-expression of β3 cDNA and inhibition of PAI-1 promotes TGFβ in human primary fibroblasts.* To confirm our findings in the PAI-1 MEFs and to show that similar results can be obtained with human cells, we utilized human primary corneal fibroblasts (HCF) to show that upregulation of β3 and knock down of PAI-1 increases TGFβ activity. HCF cells were transfected with human β3 cDNA or siRNA to human PAI-1 and co-cultured with TMLC cells. Results show that when β3 is over-expressed, TGFβ activity increased by 1.63 fold compared to vector control and that when PAI-1 synthesis is inhibited, TGFβ activity increased by 1.45 fold (Figure 6B). Over-expression of β3 (1.6 fold) and knock-down of PAI-1 (56%) was confirmed by qPCR (small panels, Figure 6B). These data confirm our findings in the PAI-1 WT and KO cells and extend our data to suggest that PAI-1 regulation of β3 to affect TGFβ activity is a general mechanism.

*PAI-1 KO cells are myofibroblasts that synthesize increased collagen.* Two markers of fibrotic disease and wound healing with scarring are the persistence of myofibroblasts and the excessive synthesis and accumulation of extracellular matrix, including collagen. To determine if PAI-1 KO cells are constitutively myofibroblasts, PAI-1 WT and KO cells were immunostained for α-SMA actin, a marker for myofibroblast differentiation. In Figure 7A, we show that the KO cells have a propensity to become myofibroblasts. To quantify collagen accumulation, the Sirius Red colorimetric assay for collagen detection was used (22). In this assay, Sirius Red dye binds to newly synthesized as well as deposited collagen and is normalized to cell number provided by Crystal violet staining. Our results demonstrate that PAI-1 KO cells consistently produce 1.6 fold more collagen than WT cells (Figure 7B). These data support the finding that PAI-1 KO cells having exaggerated TGFβ signaling and therefore are constitutively myofibroblasts that produce more ECM, in accordance with established models of fibrotic disease.

## DISCUSSION

Fibrotic myofibroblasts participate in an autocrine loop of TGFβ activation (32). Towards the goal of elucidating the mechanisms that promote enhanced TGFβ activity, we investigated the role of pro-fibrotic PAI-1 in regulating integrin αvβ3 and TGFβ activity. We discovered that the absence of PAI-1 resulted in a dramatic upregulation of total and cell surface expression of integrin αvβ3 and TGFβRII. In addition, the β3 containing focal adhesions were greatly enlarged compared to WT and resembled what is seen in myofibroblasts (2). The over-expression of endogenous β3 contributed to a 2.9-fold increase in TGFβ activity, as specifically inhibiting β3 function significantly reduced TGFβ activity. Further, over-expression of integrin β3 and knock-down of PAI-1 in human primary fibroblasts lead to a 1.63 and 1.45 fold increase in TGFβ activity, respectively, suggesting that PAI-1 regulation of β3 and resultant activation of TGFβ is a general mechanism.

αvβ3 over-expression on the cell surface may induce TGFβ activity by activating

the latent-TGFβ complex and/or by enhanced signaling through the TGFβRII. αvβ3 binds to the RGD sequence in latent-TGFβ (11) and the suggestion that αvβ3 activates latent-TGFβ on the cell surface, was derived from 1) the need to co-culture sclerodermal fibroblasts with the TMLC reporter cells to generate a TGFβ signal (suggesting that the TGFβ activity is localized to the plasma membrane and not freely diffusible) and 2) that in the presence of anti-β3 blocking antibodies the TGFβ activity was reduced by ~50% (12). We also needed to co-culture the PAI-1 WT and KO cells with the TMLC to generate a TGFβ signal. Furthermore, a β3-specific cRGD peptide reduced this activity by 59%, suggesting that αvβ3 directly activates latent-TGFβ. However, the β3 integrin may also be signaling through the TGFβRII. Because αvβ3 is not endocytosed in PAI-1 KO cells and thus remains for longer on the cell-surface, its binding to TGFβRII may be prolonged leading to enhanced signaling. The increase in TGFβ signaling would in turn upregulate synthesis of αvβ3 (12,16) resulting in an autocrine loop of TGFβ activity. Both mechanisms may work in tandem to produce a fibrotic response such as the generation of myofibroblasts and an increase in collagen synthesis as was demonstrated in Figure 7. These data are in agreement with the finding that over-expression of αvβ3 in dermal fibroblasts produced an increase in collagen α2(I) promoter activity and a blocking antibody to αvβ3, reduced synthesis of type I procollagen in sclerodermal fibroblasts (12). The TGFβRII was also upregulated in PAI-1 KO cells, which is consistent with an upregulation of this receptor in models of fibrosis when PAI-1 is over-expressed (23,24). The upregulation may be a result of enhanced TGFβ signaling, or a secondary consequence of the PAI-1 KO model. Further study is needed to distinguish between these mechanisms, however, the finding that over-expression of PAI-1 and elimination of PAI-1 both correlate with an increase in TGFβRII suggest that PAI-1 mediates TGFβRII expression levels.

Our data suggest that "normal" levels of PAI-1 are needed to avoid fibrosis. Over-expression of PAI-1 reduces PA activity leading to the accumulation of matrix and scarring. We have found that eliminating PAI-1 also promotes a fibrotic phenotype. The *in vivo* data for PAI-KO models are mixed. Some studies have demonstrated that fibrosis is ameliorated in PAI-1 KO models of kidney, liver, and lung, whereas other studies using PAI-1 KO mice have shown an increase in fibrosis in these same tissues (reviewed in (19,33,34)). Furthermore, in models of cardiac disease, over-expression of uPA and PAI-KO has consistently resulted in macrophage accumulation and cardiac fibrosis (35,36). Interestingly, one study reported that PAI-1null mice initially had reduced renal fibrosis but older mice (30 weeks) that were either null for PAI-1 or over-expressing PAI-1 (but not WT), had dramatically increased renal tubulointerstitial area, TGFβ protein and α-SMA expression, all of which are associated with renal fibrosis. The authors concluded that normal levels of PAI-1 were necessary to maintain healthy renal architecture and function in ageing (37). This study suggests that the anti-fibrotic effects of PAI-1 deficiency may be time dependent. Perhaps the initial increase in PA activity dominates in controlling fibrosis, whereas over time the over-expression of β3 and TGFβRII and the resultant increase in TGFβ produce a fibrotic phenotype.

Fibrotic healing is marked by the persistence of myofibroblasts in the wounded tissue (2,32). Myofibroblast regulation is likely to be tissue-specific as myofibroblasts in fibrotic tissue can be derived from stromal fibroblasts, EMT transition, or from fibrocytes. These differences in myofibroblast origin may contribute to the differential results reported with the PAI-KO models. The data in this study suggest that PAI-1 regulation of αvβ3 is important for maintaining normal levels of TGFβ activity and that aberrant regulation of αvβ3 by a PAI-1-mediated mechanism can result in a dramatic increase in TGFβ signaling that is associated with fibrosis. This is an important finding since several clinical therapies that target PAI-1 activity are currently under development (18,19). Our study suggests that levels of PAI-1 are critical to modulating its function, and therefore, drugs in development that reduce but not eliminate PAI-1 may

demonstrate longer-term success in preventing fibrosis.

## REFERENCES


1. Desmouliere, A., Darby, I. A., and Gabbiani, G. (2003) *Lab Invest* **83**, 1689-1707
2. Hinz, B. (2007) *J Invest Dermatol* **127**, 526-537
3. Wynn, T. A. (2008) *J Pathol* **214**, 199-210
4. Sisson, T. H., and Simon, R. H. (2007) *Curr Drug Targets* **8**, 1016-1029
5. Huang, Y., and Noble, N. A. (2007) *Curr Drug Targets* **8**, 1007-1015
6. Ragno, P. (2006) *Cell Mol Life Sci* **63**, 1028-1037
7. Czekay, R. P., Kuemmel, T. A., Orlando, R. A., and Farquhar, M. G. (2001) *Mol Biol Cell* **12**, 1467-1479
8. Czekay, R. P., Aertgeerts, K., Curriden, S. A., and Loskutoff, D. J. (2003) *J Cell Biol* **160**, 781-791
9. Nykjaer, A., Conese, M., Christensen, E. I., Olson, D., Cremona, O., Gliemann, J., and Blasi, F. (1997) *Embo J* **16**, 2610-2620
10. Blasi, F., and Carmeliet, P. (2002) *Nat Rev Mol Cell Biol* **3**, 932-943
11. Ludbrook, S. B., Barry, S. T., Delves, C. J., and Horgan, C. M. (2003) *Biochem J* **369**, 311-318
12. Asano, Y., Ihn, H., Yamane, K., Jinnin, M., Mimura, Y., and Tamaki, K. (2005) *J Immunol* **175**, 7708-7718
13. Munger, J. S., Huang, X., Kawakatsu, H., Griffiths, M. J., Dalton, S. L., Wu, J., Pittet, J. F., Kaminski, N., Garat, C., Matthay, M. A., Rifkin, D. B., and Sheppard, D. (1999) *Cell* **96**, 319-328
14. Mu, D., Cambier, S., Fjellbirkeland, L., Baron, J. L., Munger, J. S., Kawakatsu, H., Sheppard, D., Broaddus, V. C., and Nishimura, S. L. (2002) *J Cell Biol* **157**, 493-507
15. Wipff, P. J., Rifkin, D. B., Meister, J. J., and Hinz, B. (2007) *J Cell Biol* **179**, 1311-1323
16. Scaffidi, A. K., Petrovic, N., Moodley, Y. P., Fogel-Petrovic, M., Kroeger, K. M., Seeber, R. M., Eidne, K. A., Thompson, P. J., and Knight, D. A. (2004) *J Biol Chem* **279**, 37726-37733
17. Galliher, A. J., and Schiemann, W. P. (2006) *Breast Cancer Res* **8**, R42
18. Vaughan, D. E., De Taeye, B. M., and Eren, M. (2007) *Curr Drug Targets* **8**, 962-970
19. Ha, H., Oh, E. Y., and Lee, H. B. (2009) *Nat Rev Nephrol* **5**, 203-211
20. Bernstein, A. M., Twining, S. S., Warejcka, D. J., Tall, E., and Masur, S. K. (2007) *Mol Biol Cell* **18**, 2716-2727
21. Abe, M., Harpel, J. G., Metz, C. N., Nunes, I., Loskutoff, D. J., and Rifkin, D. B. (1994) *Anal Biochem* **216**, 276-284
22. Heng, E. C., Huang, Y., Black, S. A., Jr., and Trackman, P. C. (2006) *J Cell Biochem* **98**, 409-420
23. Kubo, M., Ihn, H., Yamane, K., and Tamaki, K. (2002) *J Rheumatol* **29**, 2558-2564
24. Hill, C., Flyvbjerg, A., Gronbaek, H., Petrik, J., Hill, D. J., Thomas, C. R., Sheppard, M. C., and Logan, A. (2000) *Endocrinology* **141**, 1196-1208
25. David-Pfeuty, T., and Singer, S. J. (1980) *Proc Natl Acad Sci U S A* **77**, 6687-6691
26. Roberts, A. B., Piek, E., Bottinger, E. P., Ashcroft, G., Mitchell, J. B., and Flanders, K. C. (2001) *Chest* **120**, 43S-47S
27. Lund, L. R., Riccio, A., Andreasen, P. A., Nielsen, L. S., Kristensen, P., Laiho, M., Saksela, O., Blasi, F., and Dano, K. (1987) *Embo J* **6**, 1281-1286

28. Sieuwerts, A. M., Martens, J. W., Dorssers, L. C., Klijn, J. G., and Foekens, J. A. (2002) *Thromb Haemost* **87**, 674-683
29. Srivatsa, S. S., Fitzpatrick, L. A., Tsao, P. W., Reilly, T. M., Holmes, D. R., Jr., Schwartz, R. S., and Mousa, S. A. (1997) *Cardiovasc Res* **36**, 408-428
30. Pierschbacher, M. D., and Ruoslahti, E. (1987) *J Biol Chem* **262**, 17294-17298
31. Mogford, J. E., Davis, G. E., and Meininger, G. A. (1997) *J Clin Invest* **100**, 1647-1653
32. Tomasek, J. J., Gabbiani, G., Hinz, B., Chaponnier, C., and Brown, R. A. (2002) *Nat Rev Mol Cell Biol* **3**, 349-363
33. Arteel, G. E. (2008) *J Gastroenterol Hepatol* **23 Suppl 1**, S54-59
34. Gharaee-Kermani, M., Hu, B., Phan, S. H., and Gyetko, M. R. (2008) *Expert Opin Investig Drugs* **17**, 905-916
35. Moriwaki, H., Stempien-Otero, A., Kremen, M., Cozen, A. E., and Dichek, D. A. (2004) *Circ Res* **95**, 637-644
36. Xu, Z., Castellino, F. J., and Ploplis, V. A. (2009) *Abstract, Cold Spring Harbor Meeting:XIIth International Workshop on Molecular and Cellular Biology of Plasminogen Activation*
37. Lassila, M., Fukami, K., Jandeleit-Dahm, K., Semple, T., Carmeliet, P., Cooper, M. E., and Kitching, A. R. (2007) *Diabetologia* **50**, 1315-1326



## ACKNOWLEDGEMENTS

We are grateful to to Dr. Sandra Masur and Dr. Lilliana Ossowski for their insightful comments about the manuscript, to Dr. MaryAnne Stepp for technical advice on the Sirius Red assay, and to Dr. Ralf-Peter Czekay for helpful discussions. This research was supported by NIH-NEI Grants R01 EYO17030 (AMB) and Core Grant P30-EY01867 and a Research to Prevent Blindness grant. Microscopy was performed at the MSSM-Microscopy Shared Research Facility, supported, in part, with funding from NIH-NCI shared resources grant (5R24 CA095823-04), NSF Major Research Instrumentation grant (DBI-9724504) and NIH shared instrumentation grant (1 S10 RR0 9145-01).

## FIGURE LEGENDS

**Figure 1. In PAI-1 KO cells β3 endocytosis is impaired.** (A) To confirm that PAI-1 was absent from PAI-1 KO cells, lysates were immunoprecipitated (IPed) for PAI-1 and western blotted with a second PAI-1 antibody. Loading controls demonstrate that equal quantities of the fibroblast protein, vimentin, is present in each lane. (B) β3 and early endosome antigen 1 (EEA1) co-localize in WT cells, but not in KO cells. PAI-1 WT and KO cells were incubated with FITC labeled anti-β3 antibody (green) (B, top) and FITC labeled control IgG (green) (B, bottom) for 30 min at 37°C before fixation. Cells were immunostained for (EEA1) to identify early endosomes (red). Co-localization of FITC-β3 and EEA1 is shown in WT (top left) only (yellow), demonstrating overlap. Bar=20um. (E) Percent overlap of β3 of EEA1 in each condition as determined using MetaMorph Image analysis software. Approximately 30 cells were analyzed for each condition in three independent experiments.

**Figure 2. β3 and TGFβRII expression is increased in PAI-1 KO cells.** (A) Cell surface expression: WT and KO cells were biotinylated on the cell surface before lysis and IPed for β3 or TGFβRII. Western blots were probed with streptavidin-HRP (SA-HRP) to detect biotinylated proteins.

Bands were identified by molecular weight. (B) Total expression: WT and KO cell lysates were western blotted for β3, or TGFβRII. Vimentin controls confirm equal loading (densitometry).

**Figure 3. PAI-1 KO β3-containing focal adhesions were enlarged and extended.** WT and KO cells were immunostained for β3 (A and B). Insets show enlarged images of focal adhesions (arrows). Relative focal adhesion size between WT and KO cells were quantified using MetaMorph Image analysis software (C). To demonstrate the co-localization of β3 and vinculin (a focal adhesion marker) WT and KO cells were co-immunostained for β3 and vinculin (A* and B**). To downregulate PAI-1 in WT cells, WT cells were co-transfected with PAI-1 siRNA and GFP and then immunostained for vinculin (E). GFP alone (D). PAI-1 knockdown was confirmed using Real time-PCR. (F). PAI-1 knockdown led to a similar enlargement of focal adhesions compared to non-targeting siRNA controls. (G). Bar=20um. Approximately 300 focal adhesions were analyzed in each of three experiments.

**Figure 4. SMAD 2/3 is constitutively active in PAI-1 KO cells.** (A) PAI-1 WT and KO cells were seeded on collagen (grey) or vitronectin (black) in SSFM for 24 hours (left) or SSFM plus 1ng/ml TGFβ1 for 1 hour (right). Cells were fixed and immunostained with antibodies for SMAD 2/3. Percent nuclear localization was determined by counting approximately 100 cells per condition in each of three experiments. (B) Representative images of cells seeded on collagen and quantified in (A) Bar=40um. (C) Western blots for SMAD 2 and 3 and Phosphorylated SMAD 2 and 3. Densitometry is represented by the ratio of pSMAD to SMAD that was first equalized to vinculin (pSMAD/(SMAD/vinculin).

**Figure 5. Plasminogen activator (PA) is constitutively active in PAI-1 KO cells but plasmin generation only partially accounts for the observed increase in TGFβ activity**. PA activity is not regulated by FGF-2 or TGFβ1 in KO cells. (A) PA activity was measured colorimetrically by adding a chomogenic substrate for plasmin to cell lysates. PAI-1 WT (grey) and KO cells (black) were seeded on collagen in SSFM with 1 ng/ml FGF-2 plus heparin or with 1 ng/ml TGFβ and grown for 24hrs. (B) TMLC Assay for TGFβ activity. PAI-1 MEFs were co-cultured with TMLC cells containing the luciferase gene fused to the PAI-1 promoter. Luciferase activity was measured using the Bright-Glo detection system. Where indicated, 10μg/ml aprotinin was added to the culturing media.

**Figure 6. Modulation of β3 function regulates TGFβ activity in PAI-1 KO MEFs and Human Corneal Fibroblasts**. (A) αvβ3 function was disrupted by adding a 100nM of β3-specific cyclic RGD peptide (GpenGRGD) compared to 100nM of a general RGD peptide (GRGDNP) to co-cultured PAI-1 KO and TMLC cells (see methods). TGFβ activity was quantified using the BrightGlo luciferase detection system. (B) HCFs transfected with β3 or PAI-1 siRNAs showed enhanced TGFβ activity compared to GFP or non-targeting siRNAs respectively. Quantitative qPCR confirmed β3 over-expression and PAI-1 knockdown.

**Figure 7. α-Smooth Muscle Actin expression and collagen synthesis is enhanced in PAI-1 KO cells.** (A) PAI-1 WT and KO were immunostained for α-SMA. Bar =40um. (B) Collagen accumulation was determined by staining with Sirius Red Dye (550nm). Cell numbers were determined by staining with Crystal Violet (550nm). The ratio of Sirus Red to Crystal violet was graphed.

A

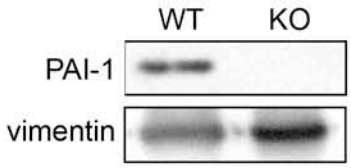


B

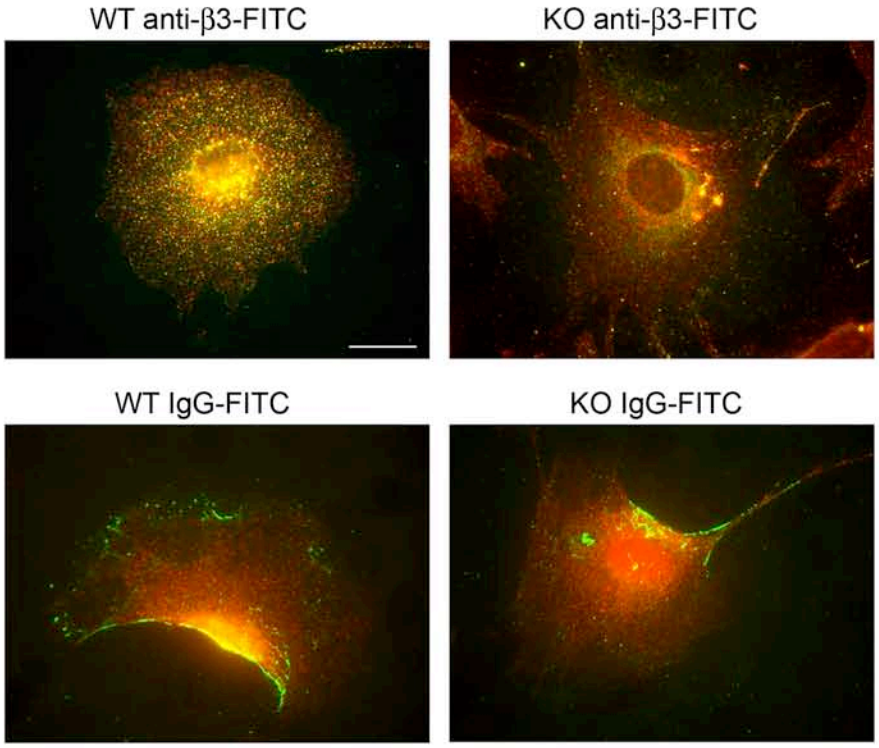


C

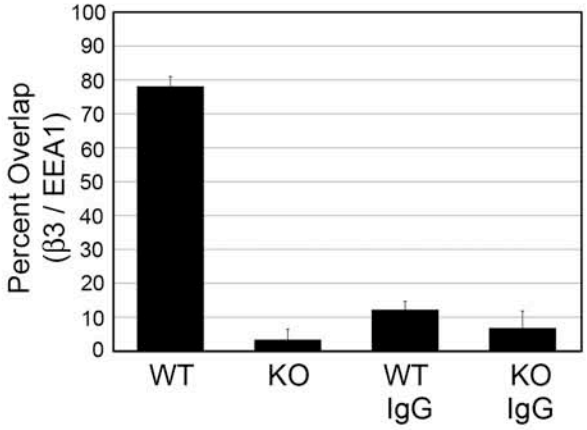


Figure 1

A

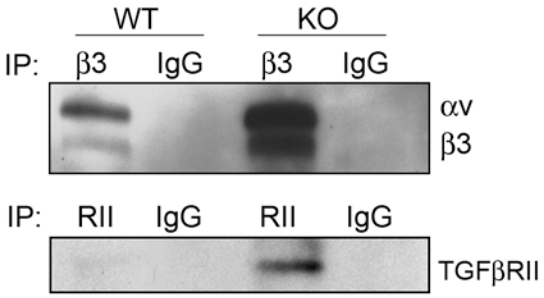


B

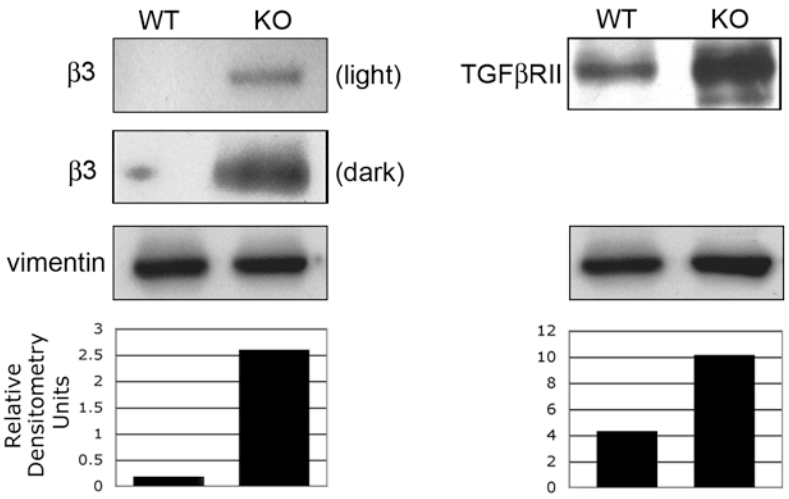


Figure 2

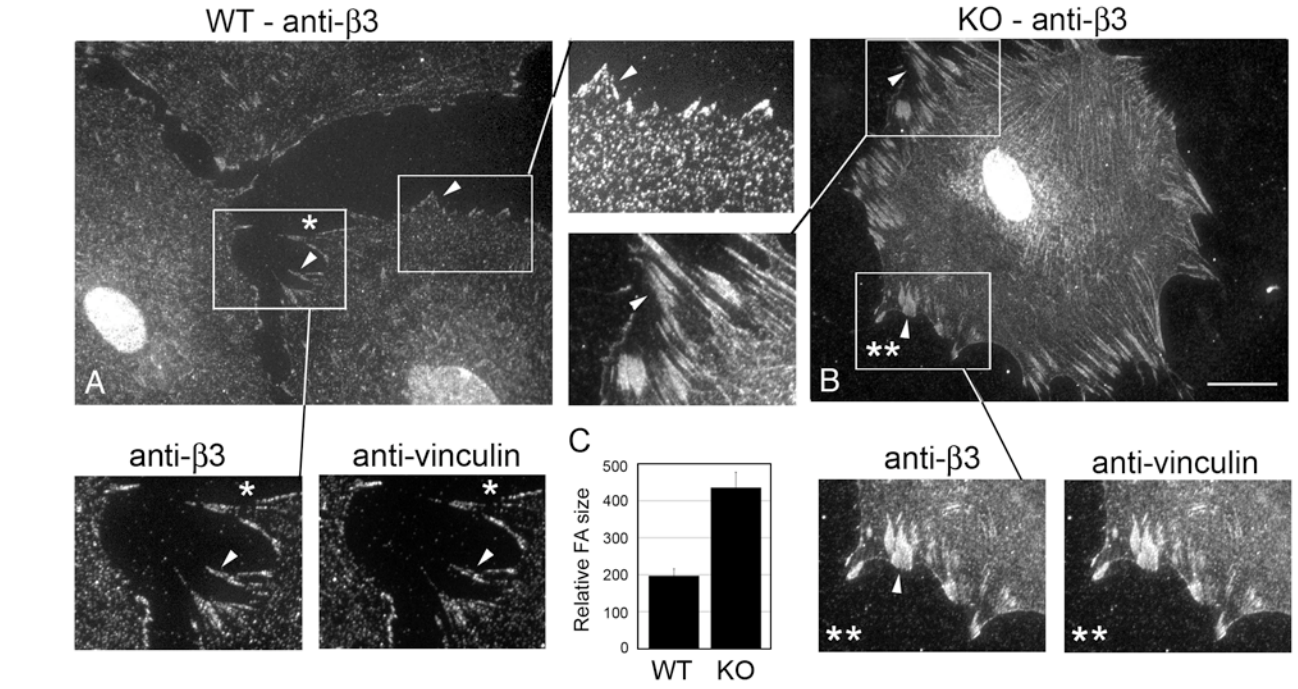


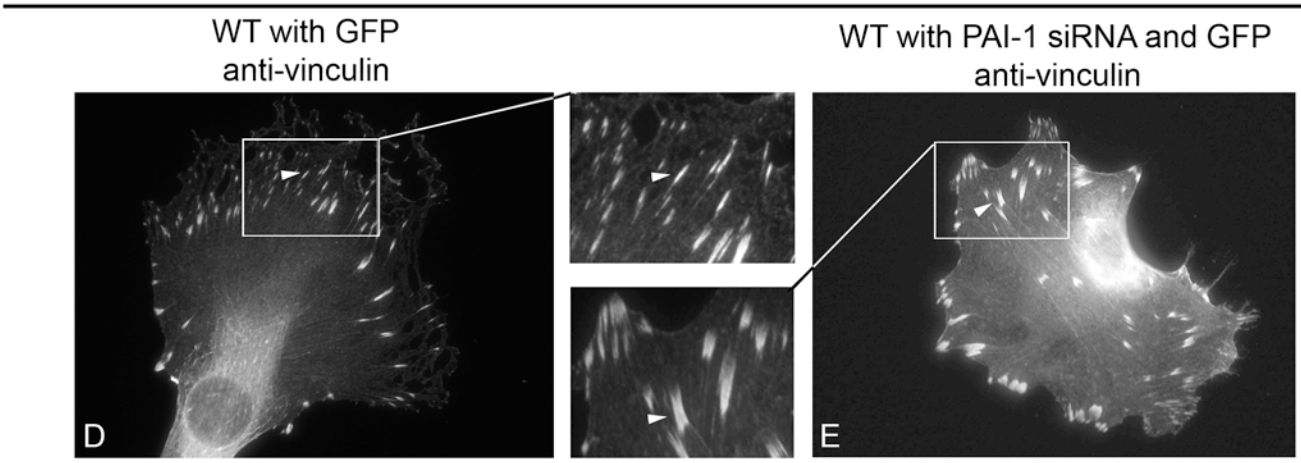


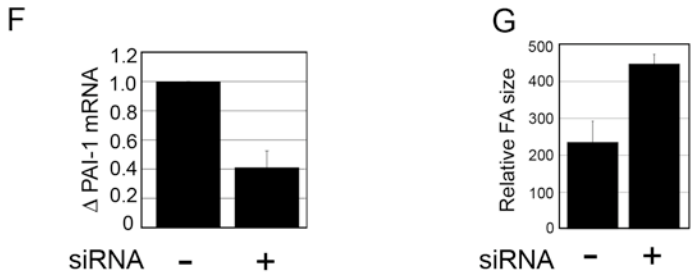





Figure 3

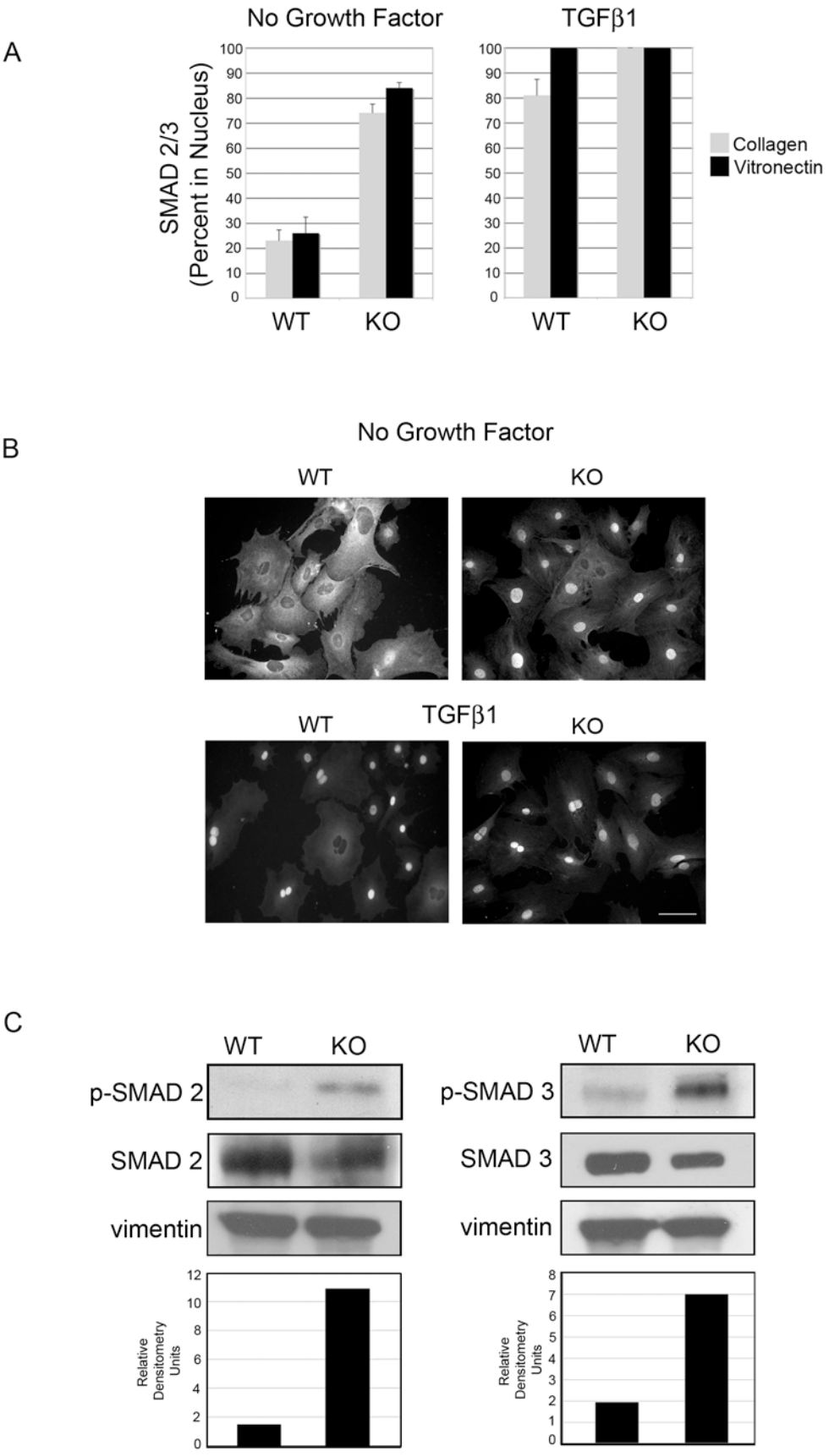


Figure 4

A

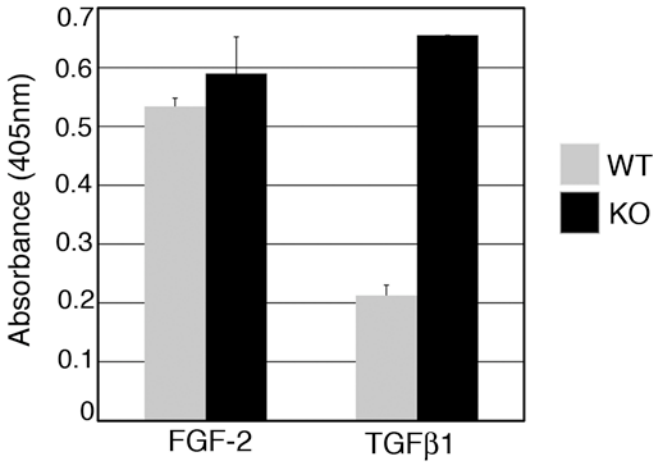


B

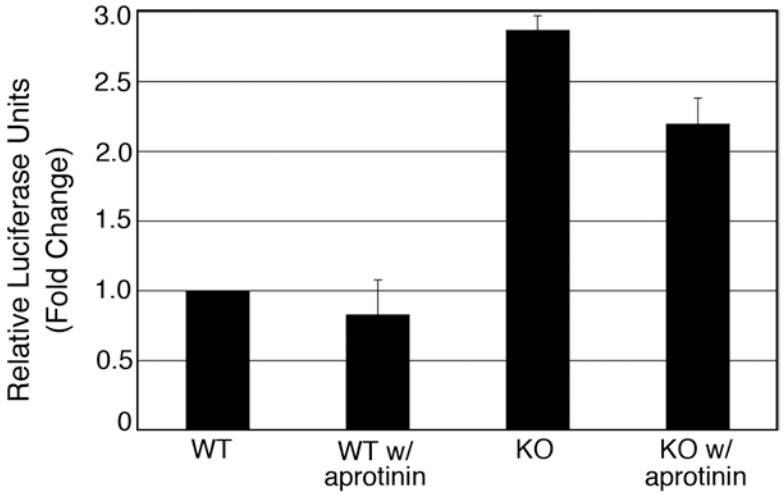


Figure 5

A

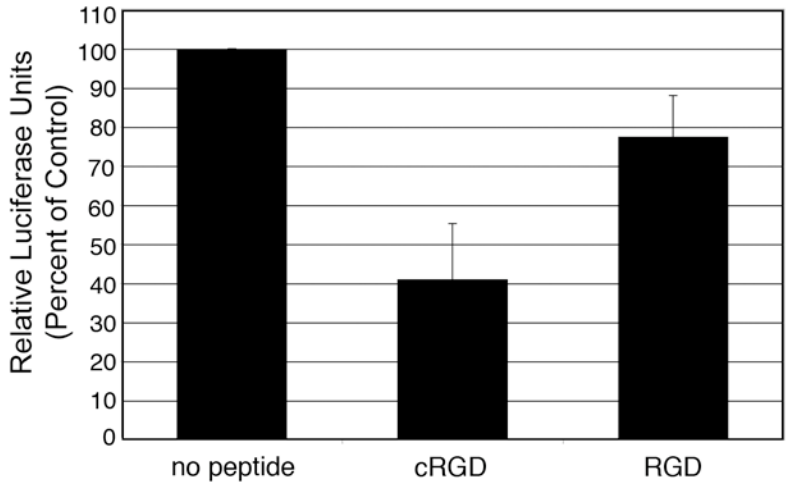


B

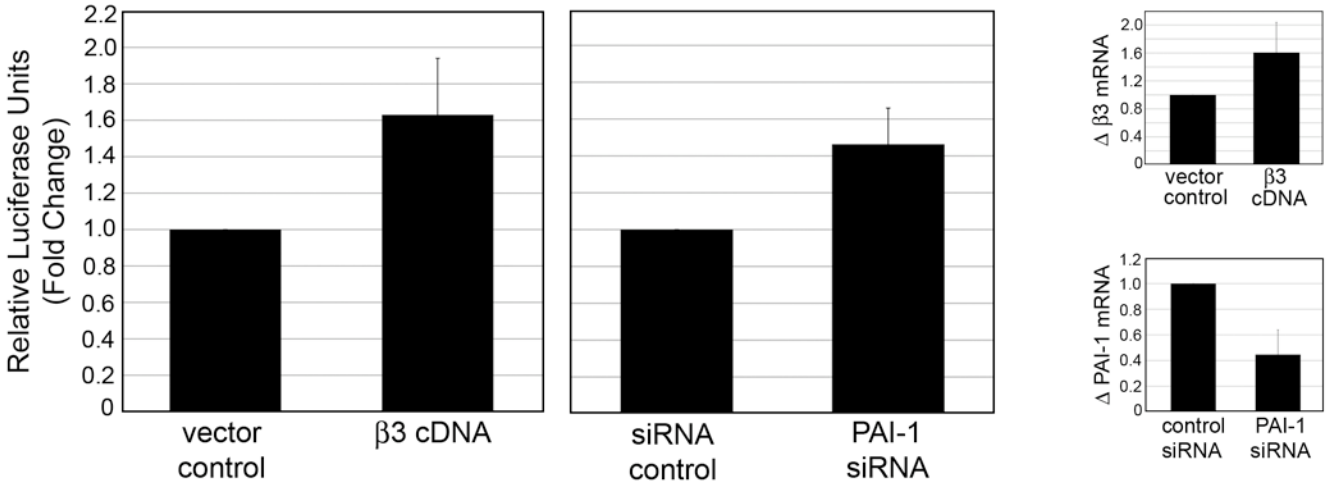


Figure 6

A

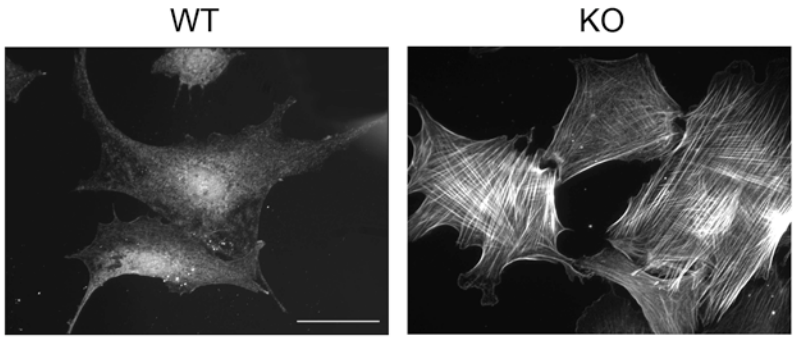


B

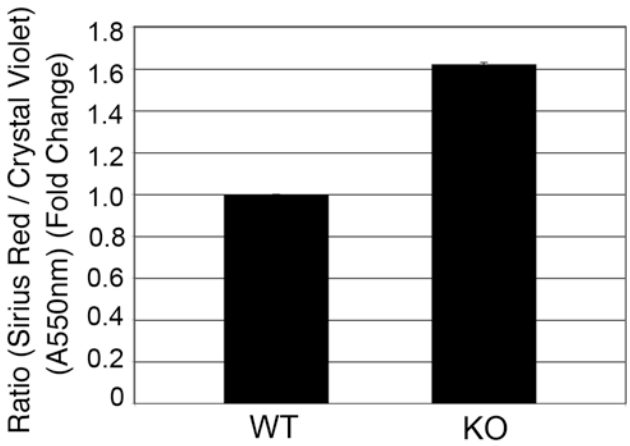


Figure 7